Available online at www.sciencedirect.com

ScienceDirect

Mendeleev Commun., 2018, **28**, 487–489

Mendeleev Communications

Template synthesis of methylammonium lead iodide in the matrix of anodic titanium dioxide *via* the direct conversion of electrodeposited elemental lead

Nikolay A. Belich,[a] Anastasia S. Tychinina,[b] Vitaly V. Kuznetsov,[c] Eugene A. Goodilin,*[b,d] Michael Grätzel[e] and Alexey B. Tarasov[a]

[a] *Department of Materials Science, M. V. Lomonosov Moscow State University, 119991 Moscow, Russian Federation*
[b] *Department of Chemistry, M. V. Lomonosov Moscow State University, 119991 Moscow, Russian Federation. E-mail: goodilin@yandex.ru*
[c] *D. I. Mendeleev University of Chemical Technology of Russia, 125047 Moscow, Russian Federation*
[d] *N. S. Kurnakov Institute of General and Inorganic Chemistry, Russian Academy of Sciences, 119991 Moscow, Russian Federation*
[e] *Laboratory of Photonics and Interfaces, Institute of Chemical Sciences and Engineering, École Polytechnique Fédérale de Lausanne, EPFL SB ISIC LPI, Station 6, 1015, Lausanne, Switzerland*

DOI: 10.1016/j.mencom.2018.09.011

A new processing technique is proposed for composites based on the hybrid organic–inorganic perovskite $MeNH_3PbI_3$ and anodic titania nanotube arrays, which includes a direct gas-phase conversion of metal lead nanorods electrodeposited inside the pores of anodic titanium dioxide. This technique may be useful for a design of solar cells and optoelectronics applications.

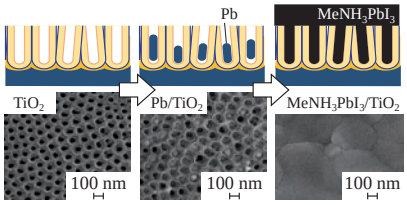

$Pb + 3MeNH_3I \rightarrow MeNH_3PbI_3 + 2MeNH_2 + H_2$

Nowadays, solar cells based on hybrid organic–inorganic perovskites attract increasing attention due to their high efficiency and potentially low production costs.[1,2] In a typical perovskite solar cell, a light-absorber film is deposited between the hole- and electron-transporting layers (HTL and ETL, respectively). The greatest power conversion efficiency of perovskite solar cell is currently achieved using a mesoporous array of TiO_2 nanoparticles as the ETL containing perovskite infiltrated into its pores.[3] This type of architecture allows one to control the crystallization of perovskite and leads to the more efficient charge carrier separation with almost no recombination of carriers.[4] A large area of TiO_2 nanostructures, such as nanorods[5–7] or anodic titania nanotubes,[8–12] with improved conductivity is considered as an alternative to mesoporous TiO_2. In this case, arrays of one-dimensional pores of anodic titania can isolate the infiltrated light absorber from the environment and enhance the stability of entire device.[13,14] In all known reports on anodic TiO_2 ETL, titanium dioxide pore filling with perovskite was performed using solution approaches. These methods of pore filling are associated with a number of difficulties in achieving complete filling of TiO_2 pores and maximizing the perovskite/TiO_2 contact area to provide better charge carriers transport between the layers.

Here, we propose a new approach for uniform filling of TiO_2 pores with perovskite. The method consists of the optimized electrodeposition of metallic lead into the pores of anodic titania with the subsequent vapor phase conversion of lead into $MeNH_3PbI_3$. Dense pore filling was achieved *via* expanding the volume of lead transformed into perovskite since the molar volume increases by the factor of 8 during the $Pb \rightarrow MeNH_3PbI_3$ direct conversion.[15] A technically similar approach was used to obtain an array of $MeNH_3PbI_3$ and $MeNH_3SnI_3$ nanorods in the matrix of anodic Al_2O_3[14–16] although aluminum oxide cannot act as an ETL in the perovskite solar cells. In addition, the reported method is not applicable for the synthesis of composites of other metals based on anodic titanium dioxide due to usual nonuniform electrodeposition of metals in the pores of conducting anodic TiO_2 films.[17,18]

In this work, the anodic TiO_2 nanotube arrays were obtained by a potentiostatic anodization of titanium foils in three steps.[†] At the second step, the anodic TiO_2 nanotube array of 500 nm thickness and 70 nm pore diameter was formed [Figure 1(*b*)], while the third step was necessary for either formation of an additional TiO_2 barrier layer between Ti foil and anodic TiO_2 nanotubes or defect healing.[18] The electrodeposition of lead[‡] was revealed to

[†] The titanium foils (BT-1 00, purity of 99.6–99.9%, thickness of 50 μm) were anodized in a two-electrode cell using an Agilent N8740A direct current source (U = 0–150 V, I = 0–22 A). At the first step, the titanium foil was pre-anodized with the following TiO_2 layer removal by 10–60 s sonication in H_2O_2 (30%) and washing with distilled water. The anodizing was carried out in ethylene glycol solution of NH_4F (0.25 wt%) and H_2O (2 wt%) at 60 V for 60 min. Then the second anodic oxidation of the titanium foil was performed in the ethylene glycol solution of NH_4F (10 g dm^{-3}) and H_2O (10 vol%) at 60 V for 75 s. A third anodizing step was performed in ethylene glycol solution of H_3PO_4 (3 wt%) at 20 V for 10 min. The resulting films were annealed at 450 °C for 1.5 h to form crystalline TiO_2 (anatase).

[‡] The deposition of lead into the pores of anodic TiO_2 films was carried out using a commercial electrolyte based on methanesulfonic acid [from Scientific and Production Enterprise (SEM.M), Russia] in the two-electrode cell in a cyclic impulse galvanostatic regime. Each cycle included a cathodic impulse (I = 100 mA cm^{-2}) of duration τ_1 and a relaxation period (I = 0 A) of duration τ_2. A multichannel potentiostat–galvanostat Biologic SAS MPG-2 was used both as a current source and recorder.

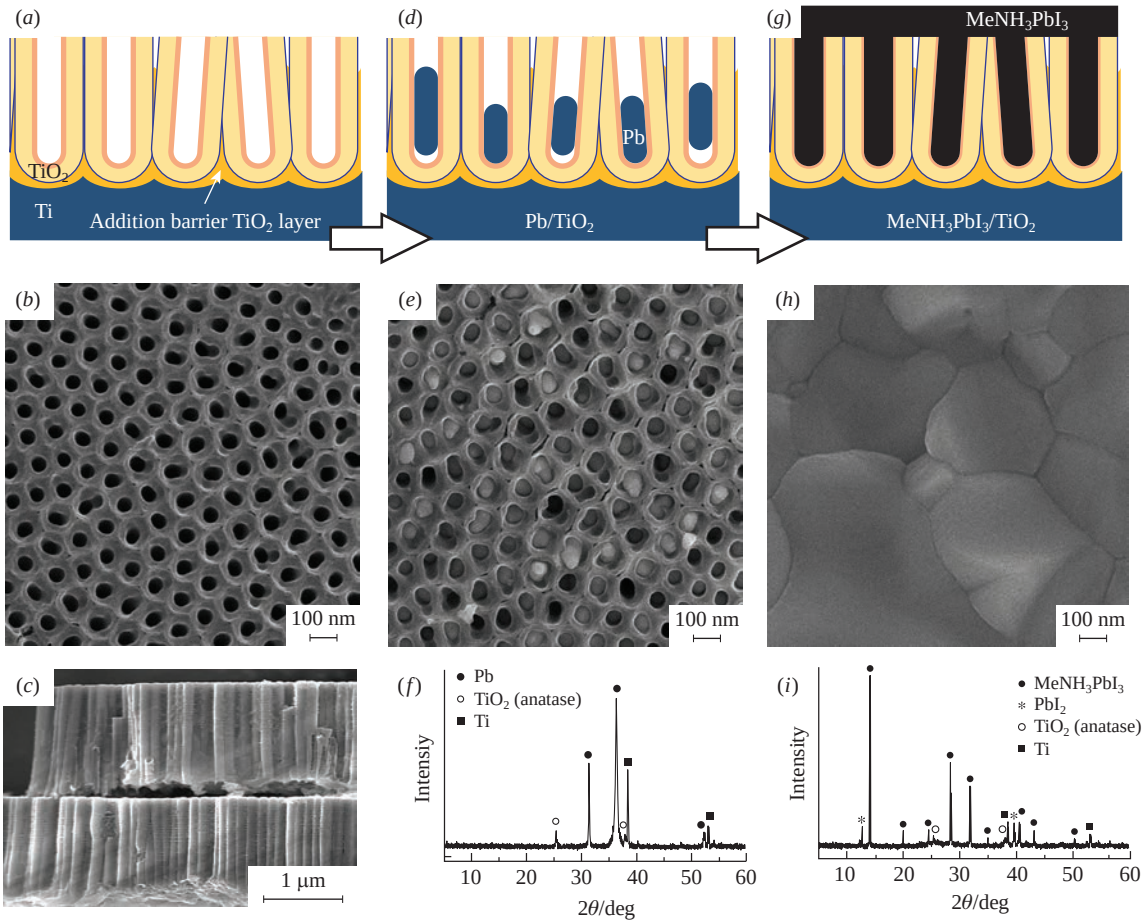

Figure 1 (*a*) A cross-section scheme of the obtained anodic TiO_2 film, (*b*) SEM of the obtained film (top view), and (*c*) SEM image of two stacked pieces of detached porous titania film demonstrating its uniform cross-section (side view); (*d*) a cross-section scheme of the obtained anodic TiO_2 film with its pores filled with metallic lead, (*e*) SEM of the obtained film (top view), and (*f*) XRD pattern of the film; (*g*) a cross-section scheme of the obtained anodic TiO_2 film with its pores filled with $MeNH_3PbI_3$ and a capping layer of perovskite, (*h*) SEM of the obtained film, and (*i*) XRD pattern of this film.

be irreproducible without the third anodizing stage due to the presence of microcracks in the thin anodic TiO_2 films. Defects, such as microcracks, provide an access for the electrolyte directly to the titanium metal substrate, which results in the deposition of metallic lead in the cracks and growth of a lead film between the Ti and TiO_2 layers. A peeling effect of anodic TiO_2 film was also observed in this scenario. The most rapid and uniform filling of TiO_2 pores with lead was achieved using $\tau_1 = 0.25$ and $\tau_2 = 7$ s (Figure S1, see Online Supplementary Materials). The use of $\tau_1 \geqslant 0.5$ s results in non-uniform pore filling and the presence of lead over the film surface, whereas $\tau_1 < 0.1$ s with $\tau_2 \geq 7$ s leads to excessive dissolution of electrodeposited lead and significantly increases the preparation time. Figure 1(*e*) shows SEM images of anodic TiO_2 film, wherein the pores were filled with metallic lead at the following electrodeposition parameters: $\tau_1 = 0.25$ and $\tau_2 = 7$ s, number of cycles $n = 3$. The X-ray diffraction pattern of the resulting film [Figure 1(*f*)] reveals the presence of metallic Pb, TiO_2 (anatase) and Ti (substrate material) phases.

Since the maximum number of photoinduced charge carriers is generated in the region of the light absorber film adjacent to the illuminated surface in the functioning solar cell, it is necessary to place the porous ETL with its pores infiltrated with the perovskite on the 'window' side for the both most rapid extraction of charge carriers and prevention of their recombination. According to this, the most crucial task is to obtain anodic $TiO_2/MeNH_3PbI_3$ composites on transparent conductive substrates, where light exposes the perovskite film through a layer of porous TiO_2, which is impossible in the case of anodic titania film obtained onto a metal foil.

The anodizing of thin titanium films deposited on glass coated with fluorine doped tin oxide (FTO) was used to create anodic TiO_2 films on transparent conductive substrates.[§] The Pb electrodeposition was carried out according to the procedure described above.

For the effective operation of a perovskite solar cell, it is necessary to eliminate short-circuiting paths between HTL and ETL layers. Consequently, a continuous capping layer of perovskite on the titania is required in addition to filling the pores with perovskite. In this study, lead electrodeposition conditions were optimized to fill the TiO_2 pores and completely cover its surface with perovskite during Pb to $MeNH_3PbI_3$ conversion (Figure S2, see Online Supplementary Materials).[¶] SEM photograph of the film surface after the completed conversion [Figure 1(*h*)] shows that $MeNH_3PbI_3$ completely covers the anodic TiO_2 film. According to

[§] A 60 nm TiO_2 barrier layer was deposited on the FTO surface prior to the deposition of the metallic Ti and its anodic oxidation to prevent the peeling off the anodic TiO_2 film during its formation and lead electrodeposition stages. A solution of titanium isopropoxide (175 μl) in absolute ethanol (2 ml) with the addition of HCl (1 μl) was spin coated onto the FTO substrate (5000 rpm, 30 s). Then the film was annealed for 30 min at 45 °C followed by DC magnetron sputtering of titanium (300 nm). Anodization was performed in the glycerol-based electrolyte (70 g dm^{-3} NH_4F, 2.5 vol% H_2O) at 20 V for 10 min.[19] The resulting films were annealed at 450 °C for 1 h.

[¶] The conversion of metallic lead into $MeNH_3PbI_3$ was carried out by the reaction of lead with gaseous methylammonium iodide. Pb/TiO_2 substrates and $MeNH_3I$ powder were placed in a flask and held at 175 °C for 1 h with constant vacuum pumping (residual pressure of ~20 mbar).

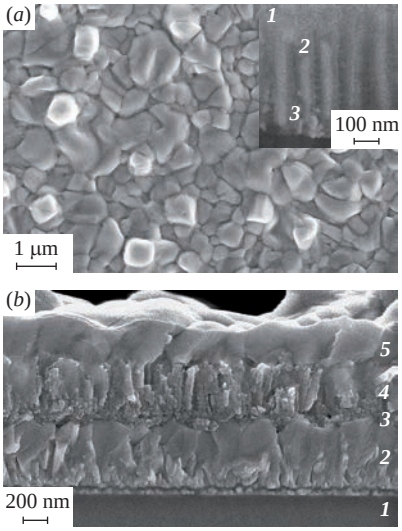

Figure 2 SEM of the obtained glass/FTO/barrier TiO_2/anodic TiO_2/$MeNH_3PbI_3$/capping $MeNH_3PbI_3$ composite: (*a*) top view with micron-sized perovskite grains, the inset shows its cross-section [(*1*) is a part of the continuous perovskite layer, (*2*) is titania nanotube array, and (*3*) is perovskite rod filling of the nanotube contrasted in the BSE mode]; (*b*) architecture of the sandwiched structure [(*1*) is glass, (*2*) is FTO conducting layer, (*3*) is titania barrier layer, (*4*) is anodic titania nanotube/perovskite nanocomposite, and (*5*) is upper layer of the perovskite grown from titania nanotubes initially filled with lead].

the XRD data [Figure 1(*i*)], a complete lead conversion occurred. The presence of PbI_2 might be attributed to a partial degradation of the film under the moist air during storage.

In the case of Pb/anodic TiO_2 films obtained on transparent conductive substrates (FTO), the conversion of metallic lead was performed under the same conditions to afford glass/FTO/barrier TiO_2/anodic TiO_2/$MeNH_3PbI_3$/capping $MeNH_3PbI_3$ composites (Figure 2).

The processing methods used in this work (anodic oxidation, electrodeposition, and annealing in the reaction medium) are potentially scalable and open up a way for the creation of large-area solar modules. A proof of concept was demonstrated here by assembling and testing Ti/TiO_2/$MeNH_3PbI_3$/Spiro-OMeTAD/carbon nanotube samples. Figure 3 shows preliminary results of measurement for such titania–carbon nanotube solar cell elements and thus reveals typical photovoltaic features of perovskite solar cells with reasonable open circuit voltage (V_{oc}), short cut current (I_{sc}), fill factor (*FF*), and still technically low effectiveness (1%).

Obviously, the application of idea of controllable template synthesis of thin continuous layers of hybrid perovskites using anodic titania nanotube arrays, for sure, makes sense (see Figure 3), suggesting that these solar cells of new type can be successfully assembled and also demonstrates operation parameters common

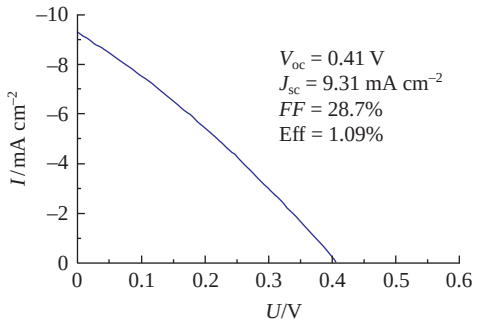

Figure 3 Photovoltaic (*V vs. I*) characteristics of the test sample of solar cell architecture Ti/anodic TiO_2/$MeNH_3PbI_3$/Spiro-OMeTAD/SWCNT measured with Keithley 2400 and AM 1.5 (Newport) certified setup. The thickness of anodic titania nanotube array template in the element is about 1 μm.

for the most of samples prepared using raw, non-optimized techniques. We strongly believe that a further progress in the adjustment and optimization of component layer thicknesses, interfaces, application of novel *n*-doped materials[20] or perovskite composition adjustment[21] will lead to much better parameters and, therefore, to an application niche of the suggested approach.

To conclude, the new potentially scalable technique has been developed for the synthesis of sandwiched structures based on the transparent conductive substrates and TiO_2 nanotube array ETL filled in the controllable manner with hybrid perovskite and the capping perovskite layer of required thickness for future application in perovskite solar cells.

This work was supported by the Ministry of Education and Science of the Russian Federation (agreement no. 14.613.21.0053 and project no. RFMEFI61316X0053).

Online Supplementary Materials

Supplementary data associated with this article can be found in the online version at doi: 10.1016/j.mencom.2018.09.011.

References

1 *NREL Best-Research Cell Efficiency Chart*, https://www.nrel.gov/pv/assets/images/efficiency-chart.png.
2 Z. Song, C. L. McElvany, A. B. Phillips, I. Celik, P. W. Krantz, S. C. Watthage, G. K. Liyanage, D. Apul and M. J. Heben, *Energy Environ. Sci.*, 2017, **10**, 1297.
3 W. S. Yang, B.-W. Park, E. H. Jung, N. J. Jeon, Y. C. Kim, D. U. Lee, S. S. Shin, J. Seo, E. K. Kim, J. H. Noh and S. I. Seok, *Science*, 2017, **356**, 1376.
4 L. Zheng, D. Zhang, Y. Ma, Z. Lu, Z. Chen, S. Wang, L. Xiao and Q. Gong, *Dalton Trans.*, 2015, **44**, 10582.
5 X. Li, S.-M. Dai, P. Zhu, L.-L. Deng, S.-Y. Xie, Q. Cui, H. Chen, N. Wang and H. Lin, *ACS Appl. Mater. Interfaces*, 2016, **8**, 21358.
6 H.-S. Kim, J.-W. Lee, N. Yantara, P. P. Boix, S. A. Kulkarni, S. Mhaisalkar, M. Grätzel and N.-G. Park, *Nano Lett.*, 2013, **13**, 2412.
7 M. Yang, R. Guo, K. Kadel, Y. Liu, K. O'Shea, R. Bone, X. Wang, J. He and W. Li, *J. Mater. Chem. A*, 2014, **2**, 19616.
8 A. Huang, J. Zhu, J. Zheng, Y. Yu, Y. Liu, S. Yang, S. Bao, L. Lei and P. Jin, *Nanotechnology*, 2016, **28**, 055403.
9 X. Wang, S. A. Kulkarni, Z. Li, W. Xu, S. K. Batabyal, S. Zhang, A. Cao and L. H. Wong, *Nanotechnology*, 2016, **27**, 20LT01.
10 X. Wang, Z. Li, W. Xu, S. A. Kulkarni, S. K. Batabyal, S. Zhang, A. Cao and L. H. Wong, *Nano Energy*, 2015, **11**, 728.
11 R. Salazar, M. Altomare, K. Lee, J. Tripathy, R. Kirchgeorg, N. T. Nguyen, M. Mokhtar, A. Alshehri, S. A. Al-Thabaiti and P. Schmuki, *ChemElectroChem*, 2015, **2**, 824.
12 P. Qin, M. Paulose, M. I. Dar, T. Moehl, N. Arora, P. Gao, O. K. Varghese, M. Grätzel and M. K. Nazeeruddin, *Small*, 2015, **11**, 5533.
13 M. J. Ashley, M. N. O'Brien, K. R. Hedderick, J. A. Mason, M. B. Ross and C. A. Mirkin, *J. Am. Chem. Soc.*, 2016, **138**, 10096.
14 A. Waleed, M. M. Tavakoli, L. Gu, Z. Wang, D. Zhang, A. Manikandan, Q. Zhang, R. Zhang, Y.-L. Chueh and Z. Fan, *Nano Lett.*, 2016, **17**, 523.
15 L. Gu, M. M. Tavakoli, D. Zhang, Q. Zhang, A. Waleed, Y. Xiao, K. H. Tsui, Y. Lin, L. Liao, J. Wang and Z. Fan, *Adv. Mater.*, 2016, **28**, 9713.
16 M. M. Tavakoli, A. Waleed, L. Gu, D. Zhang, R. Tavakoli, B. Lei, W. Su, F. Fang and Z. Fan, *Nanoscale*, 2017, **9**, 5828.
17 J. M. Macak, C. Zollfrank, B. J. Rodriguez, H. Tsuchiya, M. Alexe, P. Greil and P. Schmuki, *Adv. Mater.*, 2009, **21**, 3121.
18 N. Liu, K. Lee and P. Schmuki, *Angew. Chem. Int. Ed.*, 2013, **52**, 12381.
19 S. Berger, A. Ghicov, Y. C. Nah and P. Schmuki, *Langmuir*, 2009, **25**, 4841.
20 N. N. Shlenskaya, A. S. Tutantsev, N. A. Belich, E. A. Goodilin, M. Grätzel and A. B. Tarasov, *Mendeleev Commun.*, 2018, **28**, 378.
21 I. S. Zhidkov, A. F. Akbulatov, A. I. Kukharenko, S. O. Cholakh, K. J. Stevenson, P. A. Troshin and E. Z. Kurmaev, *Mendeleev Commun.*, 2018, **28**, 381.

Received: 21st December 2017; Com. 17/5440